Characterization of hydrothermalized zones in Pre-Salt OBN seismic data via Automatic Seismic Interpretation and Deep-learning algorithms

Leonardo Costa de Oliveira (Petrobras), Pedro Henrique Silvany Sales (Petrobras), Marcos de Carvalho Machado (Petrobras), João Adolfo Rosseto (Petrobras)

Copyright 2023, SBGf - Sociedade Brasileira de Geofísica

This paper was prepared for presentation during the 18th International Congress of the Brazilian Geophysical Society held in Rio de Janeiro, Brazil, 16-19 October 2023.

Contents of this paper were reviewed by the Technical Committee of the 18th International Congress of the Brazilian Geophysical Society and do not necessarily represent any position of the SBGf, its officers or members. Electronic reproduction or storage of any part of this paper for commercial purposes without the written consent of the Brazilian Geophysical Society is prohibited.

Abstract

Hydrothermalized zones are portions of a sedimentary basin affected by the rise of hot springs. They play a significant role in reservoir property changes, such as mineral deposition, dissolution, rock porosity and permeability, which is essential for the characterization of potentially karstified zones and geomechanical risk assessment. The dimensions of these features (which are not always within seismic resolution), and the high impedance characteristic of the Pre-Salt carbonate succession conceal lateral facies alterations, making accurate classification challenging. This study aims to improve the hydrothermalized zones characterization using a high-resolution automatic seismic interpretation combined with deep-learning algorithms in Full-azimuthal OBN data in the Barra Velha Formation from a field of Santos Basin, Southeast Brazilian margin. Automated workflow horizon interpretation was used to refine the sedimentary internal geometries. These horizons were later used as inputs to define the top and base limits for each geological target to calculate seismic facies. We applied deep convolutional autoencoders to extract seismic facies from the OBN data considering a set of Full-azimuthal pre-stack gathers as independent multi-channels. In addition, we use the student's t-distribution to create an associated facies probability map. This new strategy improved the recognition of hydrothermalized areas related to zones that registered high rates of severe fluid losses while drilling the wells. This finding has been critical not only for reservoir characterization but also for better budgetary planning of field production, such as improving the allocation of drilling rigs and fluids.

Introduction

Hydrothermal diagenetic features can increase the permeability and anisotropy of the medium in orders of magnitude, thus being able to control the hydrodynamic behavior of carbonate reservoirs, presenting production zones characterized by corridors of high permeability for the flow of fluids (Lima & De Ros, 2019). Hydrothermalism involves the circulation of hot fluids through the rocks or sediments, altering their mineralogy and chemistry (Pirajno, 2012). This process is frequently connected to areas of active volcanism (Haase et al., 2007).

In the context of the carbonate Pre-Salt deposits, the secondary porosity poses a challenge in understanding the hydrothermal features distribution due to a wide range of factors that can impact, generate, or eliminate them throughout the rock's entire developmental history (La Bruna et al., 2021). Also, magmatic events encompassing different geological periods could have triggered the liberation of significant quantities of carbon dioxide (Oliveira et al., 2023). Such an occurrence can induce karstification of the reservoir, resulting in severe circulation loss upon drilling (Oliveira, 2022) or involved in forming travertine mounds facies (Silvany et al., 2022).

Characterizing hydrothermal features requires the identification of seismic amplitude anomalies or structural discontinuities that may be the path of fluids through the basin. However, due to the high impedance values of the sedimentary carbonate fabric, identifying hydrothermal seismic facies variations in the pre-salt succession is a challenge that involves other advanced interpretation techniques that benefit from the wide azimuth and offsets acquisition ranges.

Recently, (Silvany *et al.*, 2021) showed how to apply a Deep Convolutional Auto-Encoder (DCAE) methodology to extract geological features from multi-azimuthal pre-stack seismic data, using different input channels to accommodate each azimuth and finally compute the seismic facies.

In this paper, we proposed an integrated workflow to improve the hydrothermalized zones characterization using a high-resolution automatic seismic interpretation combined with deep-learning auto-codifiers applied to Full-azimuthal OBN data from the Barra Velha Formation (BVF) in a field located in the Santos External High (SEH). The semi-automatically interpretation allowed the investigation of different azimuths contributions in the OBN seismic data. Moreover, it was possible to define geological internal geomorphology that corresponds to the top and base limits of hydrothermal zones identified by the wells. Aside from the ultra-thin stratal framework, deep convolutional codifiers extract features from azimuthal pre-stack seismic data. We propose to use Student's t-distribution to estimate the probability for each facies, and we compare the results with the areas of losses of fluids observed during drilling.

Materials and Methods

The studied area is in the Santos External High (SEH), Southeast Brazilian margin. The field is covered by a 3D seismic data survey acquired between 2019 and 2020 using the Ocean Bottom Nodes (OBN) technology. The OBN technology enables the application of the latest seismic processing and imaging technologies that benefit from the survey's full

azimuth, long offset, and broadband acquisition (Koren et al., 2011). Front-end imaging techniques include RTM and LSRTM. To generate geologically more accurate images, the model of migration velocities relied on modern FWI techniques and anisotropy calculations. According to these seismic data, the dominant frequency of the pre-salt layer is 35 Hz. Considering an estimated average velocity of 4,700 m/s from the sonic log of the well, the seismic resolution in the carbonates of the BVF is approximately 35 meters.

Multiples azimuth stack volumes, each highlighting different geological features according to the medium azimuth direction, were interpreted with the software Paleoscan. The sismostratigraphic interpretation enables to tracked horizons semi-automatically across the entire seismic volumes, chrono-stratigraphically ordered in real-time, and incorporated into the geomodeling process. Also, the method enables an interactive three-dimensional interpretation approach, allowing for a global interpretation in which changes to a given horizon alter the distribution of discontinuities around the framework automatically. This procedure accelerates and improves the generated model's accuracy significantly. The automatic surfaces extraction of the same age via the staking of horizons in the geo-model enables an ultra-thin stratal slicing of the azimuthal seismic volumes for the detection and characterization of previously unobservable geological features, which is one of the primary applications of this method. This research produced 300 horizons in the pre-salt section, of which 51 were inserted into the BVF (Figure 1).

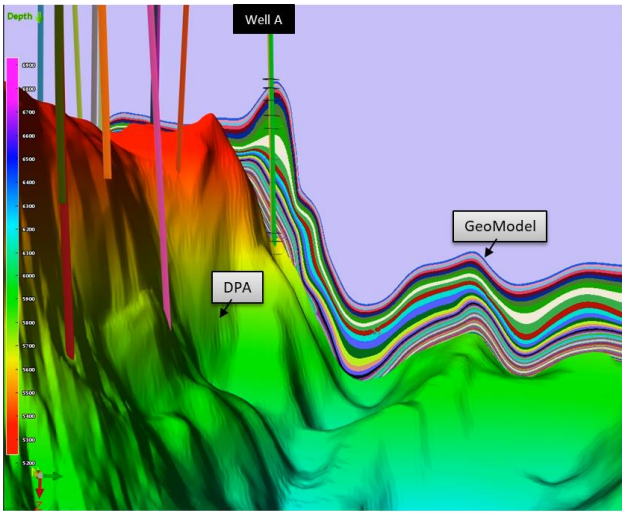

Figure 1 – Geomodel representing the ultra-thin layers in Barra Velha Formation at Well A location. DPA: Pre-Alagoas Unconformity.

With mapped horizons, it was possible to characterize facies more precisely. Furthermore, some horizons are related to the top and base limits of hydrothermally zones identified by the wells. So, we use those horizons to extract regions of interest (for instance, the window around a horizon) in the pre-stack CDP azimuthal gathers. For each point of the region of interest, time-offset panels are extracted from the input gathers by azimuths. The number of samples and offsets parametrizes the panels. Also, considering full-azimuthal data, we have one time-offset panel for each azimuth. The goal is the identification of a certain number k of facies by considering amplitude variations with azimuth effects present in the data.

We can assume that the input variables are a set of matrices $\{\mathbf{X}i, i=1...N\}$ in the space, where $N1$ is the number of time samples, and $N2$ is the number of offsets. Then, to identify the facies, we can treat each matrix $\mathbf{X}i$ as a vector and apply a clustering method over this set of vectors. Clustering means aggregating the vectors in a number k of collections according to certain similarities.

The vectors created by those panels are in a high vector space. Clustering involves work with distances between vectors, but these computations are no reliable in this case due to the space dimensionality. This kind of problem is known as “curse of dimensionality” (Bellman, 1961). So, a dimensionality reduction process is applied before clustering.

It is used an artificial neural network, the Deep Convolution Autoencoder (DCAE). This kind of network learns efficient data encodings. The network is composed by two subnets, the encoder and the decoder (Figure 2). The training aims to compute the network weights that permits the network encode and reconstruct each input panel (it is an unsupervised learning method). The input panels are treated as 2d images and each azimuth is mapped in a different channel of the images.

DCAE is implemented using the denoising autoencoders (Vincent et al., 2008) strategy: it learns to approximate the original input by training on the input vectors with noises. The DCAE is designed to reconstruct the original data from the corrupted version of the original images, forcing the hidden layer to discover more robust features and preventing overfitting noises. Figure 2 shows schematically the structure of DCAE.

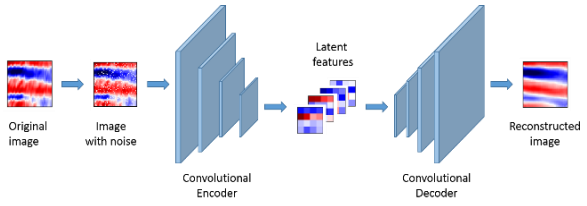

Figure 2 - The structure of DCAE.

Once trained the network (the first step of the method), the encoder subnet is used to generate a code vector (latent features with low dimensionality) for each input panel. The codes are then submitted to a clustering algorithm. Also, in order to evaluate the probability of each point belonging to each cluster, we adopt the Student t-distribution, following the classical work of (van der Maaten & Hinton, 2008).

The Figure 3 describes the second step: the set of multi-azimuthal panels are submitted to the encoder, the set of codes are then clustered generating the facies map, the probability map and the centroid image for each facies. More details on the method used to extract the facies from prestack can be found in (Silvany et al., 2019, 2021).

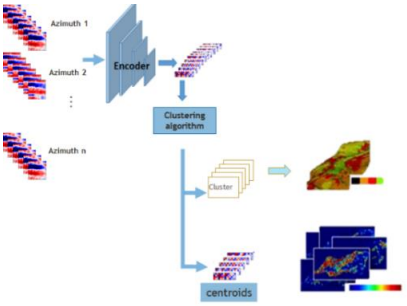

Figure 3 - The second step of the method.

Reservoir Case Study

In the studied area, the BVF (i.e., sequences K44 and k46K48 – cf., Moreira et al., 2007) represents the main reservoir, occurring both in situ facies (shrubs, claystone, and spherulites) and reworked facies (grainstones, rudstones, and wackstones) (cf. Gomes et al., 2020).

The mound features are the main reservoirs. They occur in locations both proximate to the edge faults (Figure 4) and distal from the structural highs (where it exhibits a backstepping geometry). They have a narrow, elongated external geometry and a rounded to pointed top (mainly in the K46-K48 sequence). Internally, the mounds show chaotic seismic facies, alternating discontinues reflectors with subparallel a continuous shape. This seismic characteristic differentiation is mainly due to the seismic acquisitions and processing improvement in the area.

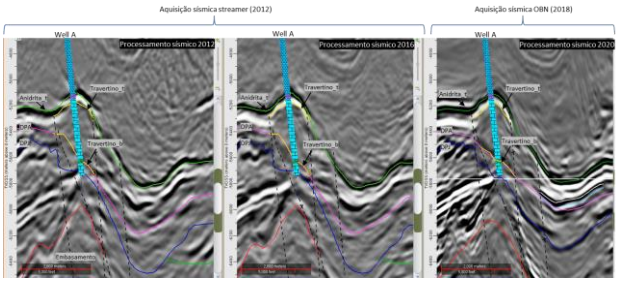

Figure 4 – Seismic sections show different data acquisitions and processing at well A location. The first seismic profiles refer to a Streamer seismic acquisition in 2012, with a single N-S survey direction (Narrow Azimuth). The second image refers to a reprocessing of the same acquisition. The third section is from the OBN (Ocean Botton Nodes) acquisition with the full azimuth technique. Notice that different geological features became progressively better imaged with the seismic data evolution over time.

Furthermore, the OBN seismic data inversion reveal low impedance values and high lateral continuity in the mounds area (Figure 5). These are features of high permo-porosity, where significant losses of fluids were observed during drilling (accumulated losses greater than 6000 barrels, with severe loss rates of around 150 barrels per hour in some wells). The challenge associated with severe loss forecasting in Pre-Salt reservoirs arises from the disparity between the seismic facies that are possible to identify and the occurrence of rapid facies variations that are typical of this depositional context. A limited quantity of high impedance reflectors has been generated because of this characteristic, which hides most of the fluctuations. This way, single seismic facies may correspond to distinct situations, one of which may have experienced significant circulation loss while the other did not. This issue represents just one of the challenges that may arise in the utilization of neural networks for pre-salt rock analysis.

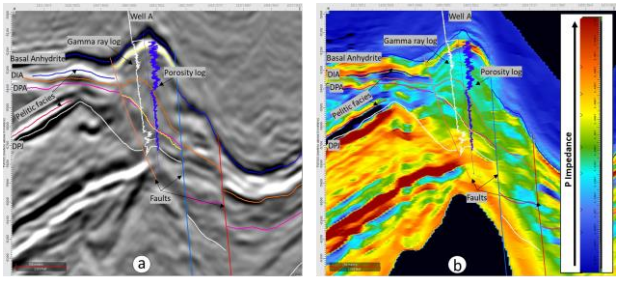

Figure 5 – Travertine mound geological feature in the studied area. a) Seismic section in amplitude. b) same section visualized with impedance P. Note that the mound is characterized by low impedance values, represented in blue color variations.

With higher frequency gain and information from different azimuths in the OBN data (Figures 4; 5), it was possible to build an accurate geomodel concerning the seismic geomorphology and, consequently, extract internal horizons in the mound correlated with the hydrothermal features described in the drilled wells (Figure 6). This step allowed the recognition of different reservoir zones from a high-resolution stratigraphic slicing.

The map in Figure 7 shows the seismic facies obtained with DCAE method applied over sixteen pre-stack CDP gathers. According to one potential interpretation of this map, purple and blue seismic facies occur at the structure's margins and are closely associated with the main fault to the east. It also occurs in the southern portion in the structural lows, always with strong parallelism with the structural fabric of the area, with NNE-SSW variations. On the other hand, seismic facies represented by the color's navy blue, red and white facies are notoriously concentrated inside the structure, specifically in its center. These seismic facies are separated from the previous ones by a regional structure with NNW-SSE and NWW-SEE variations. When we compare these seismic classes with fluid loss data from the operation of the wells, it is observed a strong association between the seismic class purple and blue with the greater loss of fluids areas in the studied field (red balls). Similarly, the wells with the lowest loss volume are associated with navy blue, red and white facies.

Conclusions

The semi-automatically interpretation allowed the investigation of different azimuths contributions in the OBN seismic data (Figures 4; 5). Furthermore, it was possible to build an accurate model concerning the internal seismic geomorphology and generate horizons corresponding to mound hydrothermal features described in the wells. Aside from the ultra-thin stratal

framework, deep convolutional codifiers extract features from altogether azimuthal pre-stack seismic data with a high level of abstraction and in a non-linear way.

Using these features as input to a clustering method, a seismic facies map can be generated from pre-stack data. In contrast to conventional methodologies, the findings indicate better precision in identifying hydrothermal regions and architectural elements associated with this phenomenon, such as mound structures.

The probability maps obtained with different strategies also supported the uncertainty analysis of the depositional facies in geological modeling, including the identification of two distinct seismic classes associated with regions with different patterns of drilling fluid loss.

Apart from the economical outcomes that have already been integrated into the routine operation of the field wells, this study holds the capacity to enhance the strategizing of exploration and development wells across diverse regions of the Pre-salt.

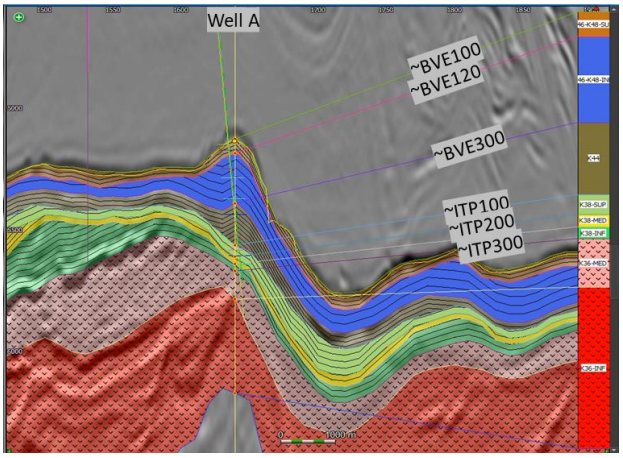

Figure 6 – Ultra-thin seismic stratal framework inside the travertine mound. Notice that was possible to individualize different reservoir zones in high resolution. From the geo model created, only 50 horizons were generated in the BVF (i.e., sequences K44, K46K48).

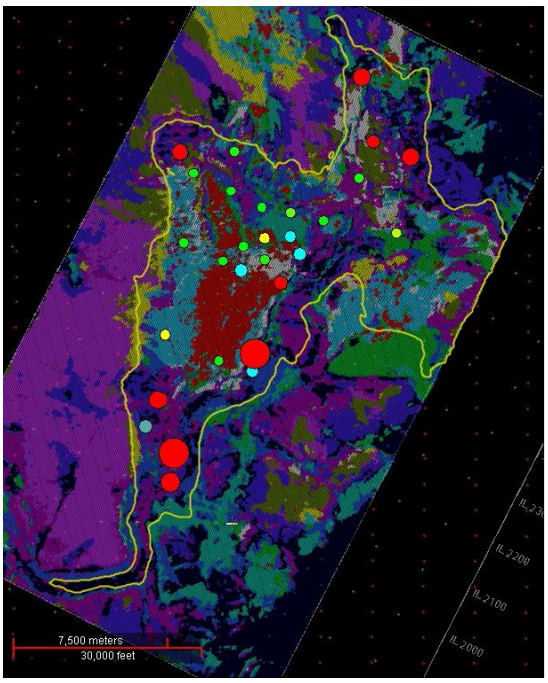

Figure 7 – Seismic facies obtained with DCAE methodology applied over sixteen pre-stack CDP gathers. The circles sizes are associated with accumulated losses barrels in the well's areas.

Acknowledgments

We thank Petrobras for permission to publish this work.

References

Bellman, R. Adaptive Control Processes: A Guided Tour. Princeton University Press, Princeton, New Jersey, 1961.

Gomes, J.P., Bunevich, R.B. Tedeschi, L.R. Tucker, M.E. and Whitaker, F.F., 2020. Facies classification and patterns of lacustrine carbonate deposition of the Barra Velha Formation, Santos Basin, Brazilian Pre-salt, *Marine and Petroleum Geology* 113, 104176, doi: 10.1016/j.marpetgeo.2019.104176.

Haase, K. M., Petersen, S., Koschinsky, A., Seifert, R., Devey, C. W., Keir, R., ... & Weber, S. (2007). Young volcanism and related hydrothermal activity at 5° S on the slow-spreading southern Mid-Atlantic Ridge. Geochemistry, Geophysics, Geosystems, 8(11).

La Bruna, V., Bezerra, F. H., Souza, V. H., Maia, R. P., Auler, A. S., Araujo, R. E., ... & Sousa, M. O. (2021). High-permeability zones in folded and faulted silicified carbonate rocks–Implications for karstified carbonate reservoirs. Marine and Petroleum Geology, 128, 105046.

Lima, B. E. M., & De Ros, L. F. (2019). Deposition, diagenetic and hydrothermal processes in the Aptian Pre-Salt lacustrine carbonate reservoirs of the northern Campos Basin, offshore Brazil. Sedimentary Geology, 383, 55-81.

Koren Z. and Ravve I. [2011] Full azimuth subsurface angle domain wavefield decomposition and Imaging Part 1 and 2. Geophysics 76(1), S1-s13.

Moreira, J.L.P. Madeira, C.V. Gil, J.A. and Machado, M.A.P. 2007. Bacia de Santos. *Boletim de Geociências da Petrobras* 15(2), p. 531–549.

Oliveira, C. L. (2022). Influence of the Magmatism on Severe Loss Events in the Mero Field, Santos Basin, Brazil. In Fourth HGS/EAGE Conference on Latin America (Vol. 2022, No. 1, pp. 1-4). EAGE Publications BV.

Oliveira, L. C. D., Penna, R. M., Rancan, C. C., Carmo, I. D. O., & Marins, G. M. 2023. Seismic Interpretation of the Mero Field Igneous Rocks and its Implications for Pre- and Post-Salt CO2 Generation – Santos Basin, Offshore Brazil. Available at SSRN: https://ssrn.com/abstract=4394061 or http://dx.doi.org/10.2139/ssrn.4394061 .

Pirajno, F. (2012). Hydrothermal mineral deposits: principles and fundamental concepts for the exploration geologist. Berlin: Springer.

Silvany, P., Machado, M., Matos, M., Paes, M., Joint multi-azimuthal pre-stack and time-frequency attributes seismic facies prediction via Deep learning: an application to a Brazilian Pre-salt reservoir. SEG Annual Meeting (2021).

Sales, P. S., Machado, M. D. C., & Bunevich, R. B. (2022, June). Quality Uncertainty Analysis of Travertine Architectural Elements Associated to Lacustrine Carbonate Deposits Via Deep Transfer Learning. In *83rd EAGE Annual Conference & Exhibition* (Vol. 2022, No. 1, pp. 1-5). EAGE Publications BV.

Van der Maaten, L., & Hinton, G. (2008). Visualizing data using t-SNE. *Journal of machine learning research*, *9*(11).

Vincent P., Larochelle H., Bengio Y., and Manzagol P.-A., “Extracting and Composing Robust Features with Denoising Autoencoders,” Proc. Int’l Conf. Machine Learning, 2008.